Journal of Materials and Environmental Science
ISSN : 2028-2508
e-ISSN : 2737-890X
CODEN : JMESCN

J. Mater. Environ. Sci., 2025, Volume 16, Issue 9, Page 1709-1720

http://www.jmaterenvironsci.com

Evaluation of the physico-chemical properties of two clays for use as adsorbents in wastewater treatment

Ibrahima SAKO[1], Alfred Niamien KOUAME[2*], Diby Benjamin OSSONON[1], Kacou Charles KINIMO[1], Bi Irié Hervé GOURE DOUBI[1]

[1]Training and Research Unit of Biological Sciences, Department of Mathematics, Physics and Chemistry, Peleforo GON COULIBALY University, BP 1328 Korhogo, Côte d'Ivoire
[2]Laboratory of Constitution and Reaction of Matter (LCRM), Félix Houphouët-Boigny University, 22 BP 582 Abidjan 22, Abidjan, Côte d'Ivoire

**Corresponding author, Email address: kouame.alfred2@ufhb.edu.ci*

Received *10 June 2025,*
Revised *04 Sept 2025,*
Accepted *06 Sept 2025*

Keywords:
- ✓ *Clays;*
- ✓ *Physico-chemical properties*
- ✓ *Adsorbents;*
- ✓ *Wastewater treatment;*

Citation*: Sako I., Kouame A.N., Ossonon D.B., Kinimo K.C., Goure Doubi B.I.H. (2025) Evaluation of the physico-chemical properties of two clays for use as adsorbents in wastewater treatment, J. Mater. Environ. Sci., 16(9), 1709-1720.*

Abstract: This study is a contribution to the valorization of local clays in wastewater treatment by adsorption. Two clays, one noted AG-Kor from Korhogo in the North andthe other AG-Ya from Yaou in the South of Côte d'Ivoire were subjected to physico-chemical and mineralogical characterization to determine their properties. The results of the chemical analyses by ICP and X-ray diffraction showed that the samples are mainly composed of kaolinite (47.15% for AG-Kor and 21.53% for AG-Ya) and quartz (25.07% for AG-Kor and 49.71% for AG-Ya), with associated iron compounds of 8.9% for AG-Kor and 6.3% for AG-Ya, respectively. The particle size determined by the DLS method revealed that the samples were fine, with an average particle size of 0.5132 µm for AG-Kor and 0.7272 µm for AG-Ya with around 72% micropores. As for the specific surface area evaluated by the BET method, tests revealed quite large specific surfaces for both samples with 42.04 and 33.68 m^2/g respectively for AG-Kor and AG-Ya. All these results show that both samples have good chemical reactivity and can therefore be used as adsorbents in wastewater treatment.

1. Introduction

Environmental pollution is one of the major development problems. Indeed, human activities impact the environment through different forms of pollution that affect several essential environments of life including air, water and soil. Water, an indispensable element for life, is contaminated by pollutants that alter its composition and degrade its quality, which makes its use risky for humans and the ecosystem. These pollutants come from a variety of sources, the main ones being transport, industry and agriculture, affect both surface water and groundwater, thus compromising their availability and health (Abbès, 2017).

Several treatment processes for decontamination exist but are very expensive for developing countries and show their limits because they are often faced with species poorly biodegradable or

refractory to chemical oxidants (O_3, Cl_2,…) and may induce secondary or parasitic reactions (Rodier, 2005; Razzouki *et al.*, 2015, Azzaoui *et al.*, 2024). These techniques include electrochemical processing, membrane filtration technology, etc. Other less treatment techniques such as adsorption are being developed. Adsorption is a physical or chemical phenomenon by which molecules present in a liquid or gaseous effluent bind to the surface of a solid. This process uses adsorbents such as activated carbons (Balogoun *et al.*, 2015; Jebahi *et al.*, 2022), zeolites (Ünnü *et al.*, 2016; Rache *et al.*, 2014) silica gels (Martinez *et al.*, 2007) and clays (Bel Hadjltaief *et al.*, 2014; Ayari *et al.*, 2004 ; Akartasse *et al.*, 2022). The performance and efficiency of the adsorption technique are largely related to the nature of the adsorbent, its cost, its abundance and its regeneration. As a result, the search for less expensive, readily available, easily usable and effective adsorbents has directed researchers to natural materials such as clays. Clays are exceptional nanoparticles due to their reactivity and abundance. Their nanometric size and leaf-like structure give them a specific surface area that enables them to effectively retain many pollutants, whether they are of natural or anthropogenic origin (Bensid, 2016; Jodeh *et al.*, 2018; Hamed *et al.*, 2019; Deghles, *et al.*, 2019).

Côte d'Ivoire is full of many clayey and lateritic materials that are increasingly valued in several fields including Compressed Earth Bricks, bioplastics and in the depollution of contaminated water with quite satisfactory results (Kouadio *et al.*, 2024; Kouamé *et al.* 2021; Méité *et al.*, 2021). In view of their abundance and the fairly satisfactory results obtained from previous studies, two local clays will be the subject of this study with a view to their valorization in waste water treatment.

2. Raw materials and experimental techniques

2.1 Clay samples

The clay samples used in this work were collected from two towns (Korhogo and Yaou) in Côte d'Ivoire. The sample designated AG-Kor was taken in the town of Korhogo in the northern region of the country, at coordinates 9°26.930' N and -5°-38.936' E. This clay is a reddish colour (**Figure 1a**). The second yellowish sample (**Figure 1b**), marked AG-Ya, comes from the town of Yaou in South-Eastern part of Côte d'Ivoire, at coordinates 08°08.42'N and 005°06.125'O.

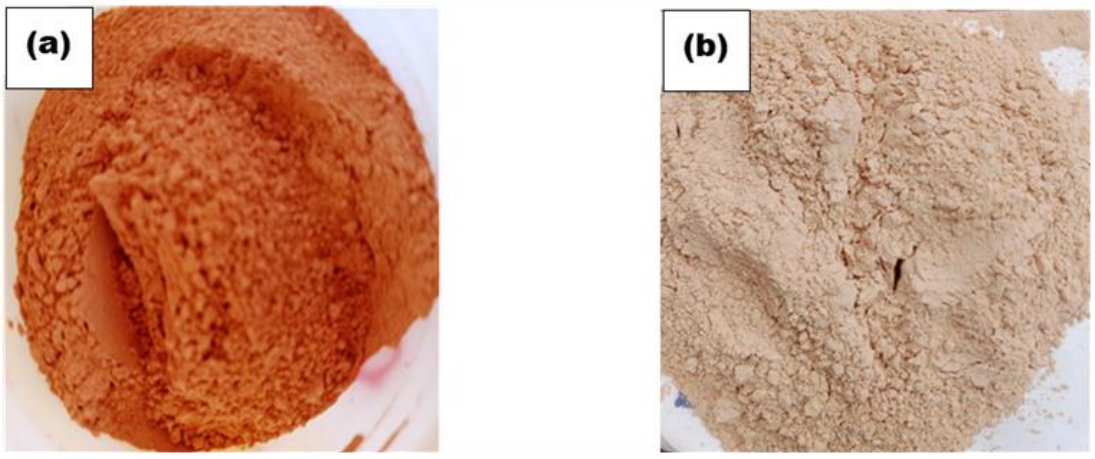

Figure 1. Clay samples: (a) AG-Kor ; (b) AG-Ya

Before carrying out the various characterization tests, samples were dried in the sun for three days to reduce humidity and then crushed with a porcelain mortar. The powder obtained was then sieved using a 100 µm mesh sieve (SAULAS ISO 3310) and stored in hermetic jars.

2.2 Experimental techniques

This paragraph summarizes all the experimental techniques used to evaluate the physico-chemical and mineralogical properties of the two samples, properties which are essential before any prospect of adding value to these raw materials.

The particle size and zeta potential of the samples were determined by the DLS (Dynamic Light Scarttering) method. The Zetasizer Nano ZS type device (Malvern, Zetasizer nano S90) was used for the different measurements. The average particle size was taken from a total of 15 measurements at 25°C for each sample.

The Brunauer, Emmett and Teller (BET) method was used to characterize the texture of powdered solids. To do this, the samples were degassed in a vacuum at 200°C for 4 hours. Next, an automated volumetric nitrogen adsorption apparatus type TMAXCN (TMAX-BSD-PM2) using nitrogen multilayer adsorption at 77 K was used to perform the measurements.

The elemental chemical composition of the clays was determined by Inductively Coupled Plasma-Atomic Emission Spectrometry (ICP-AES) using a Thermo Fisher-type spectrometer using an argon plasma (10,000 K).

X-ray diffraction (XRD) was used to identify the crystalline phases of clays. The diffractometer used is Bruker D8 Advance x-ray θ/2θ with Cu-Kα radiation (λ = 1.542 Å).

The quantitative mineralogical composition was obtained from the results of chemical composition determined by ICP and qualitative mineralogical composition revealed by XRD. To do this, the following **equation 1** is applied:

$$T(a) = \sum M_i \text{ x } P_i(a) \qquad \textbf{Eqn.1}$$

With:

T(a): Content (%) of the element a in the material,

M_i: Content (%) of mineral i in the material,

Pi(a): Proportion of the element a in mineral i.

Infrared spectra of the samples were obtained using a Fourier Transform Infrared (FTIR) spectrometer (Nicolet 6700 / Smart iTR) coupled with an ATR (Single Reflection Attenuated Total Reflectance) device equipped with a diamond crystal (Type IIa Diamond, 45°, 2 mm × 2 mm, penetration depth of 2.0 µm).

Scanning electron microscopy coupled with X-ray energy dispersive analysis (SEM-EDX) was used to observe the surface of adsorbents in order to see the state of their surfaces and to highlight the main chemical elements present on their surfaces. The tests were carried out using a Tescan LYRA 3 XMH electron microscope equipped with an energy-dispersive (EDX) QUANTAX Compact X-ray detector (X-Flash 6160).

The thermal behaviour of the samples was studied using TA Instruments® TGA (Q500)/ Discovery® MS under a constant air flow of 90 ml/min, from 30 to 900°C with a temperature rise rate of 5°C/min.

3. Results and Discussion

The average particle size and zeta potential values of the two clay samples, AG-Kor and AG-Ya, are presented in **Table 1.**

Table 1. Average particle size and zeta potential of adsorbents

Properties	Adsorbents	
	AG-Kor	AG-Ya
Average particle size (µm)	0,5132	0,7272
Zeta Potential (mV)	-16,7	-19,62

The particle size results show that both samples are fine, with an average particle size of less than 1µm. This fine particle size predicts the presence of large quantities of clay minerals in these two samples. The zeta potential values of -16.7 mV for AG-Kor and -19.62 mV for AG-Ya show that the samples have an overall negative surface charge, which can be explained by the negative charges on the clay mineral sheets. In general, dispersion stability depends of charge amplitude, not sign. The charge amplitudes of the AG-Kor (16.7 mV) and AG-Ya (19.62 mV) samples are between 10 and 20 mV. For such dispersions, stability is said to be limited, and coagulation is likely to occur due to the forces of inter-particle attraction dominating over the forces of repulsion.

The specific surface area values of AG-Kor and AG-Ya clays determined by the BET method are 42.04 and 33.68 m^2/g, respectively. These high values could be explained by the fineness of the samples according to the granulometry results which showed an average particle size of less than 1µm. Indeed, the particle size of a soil is a key factor that influences the specific surface area, so the finer the soil, the larger its specific surface area (Feller *et al*., 1992). In addition, the surface areas obtained are larger than those of kaolinitic clays, generally between 10 and 30 m^2/g, which may suggest, on the one hand, the presence of other clay minerals such as illite and, on the other hand, the presence of iron compounds that could contribute to the increase in the specific surface area (Sei *et al*., 2002; Soro, 2003). As for the volume of the micropores of 0.015 and 0.012 cm^3/g respectively for AG-Kor and AG-Ya, it is of the same order as that of the kaolinite minerals (0.01-0.05 cm^3/g). All these textural properties show that these two samples AG-Kor and AG-Ya will have a good chemical reactivity and therefore can be used in the adsorption of pollutants.

Table 2. Textural properties

Properties	Adsorbents	
	AG-Kor	AG-Ya
Specific Surface area BET (m^2/g)	42.04	33.68
Micropore volume (cm^3/g)	0.015	0.012
Microporosity percentage (%)	72.95	72.12

The chemical composition of the clays is recorded in **Table 3**. The results obtained indicate that both clay samples are essentially composed of silicon oxide (SiO_2), aluminum (Al_2O_3) and iron (Fe_2O_3). These two clays can therefore be classified in the group of aluminosilicates because of the high content of silicon oxide and aluminum (Manouan *et al*., 2024). The SiO_2/Al_2O_3 ratio of 2.51 for AG-Kor and 5.84 for AG-Ya is higher than that of pure kaolinite, which is generally between 1 and 2. Therefore, this difference could be explained by the presence of free silica potentially in the form

of quartz in the clay fraction (Qlihaa *et al.*, 2016). The higher value for AG-Ya would indicate an excess of silica in this sample. In addition to major oxides, both samples contain potassium oxides (K_2O) and rutile (TiO_2) in small quantities. Loss on ignition values of 20.54% and 13.97% for AG-Kor and AG-Ya respectively are relatively high and may be attributed to dehydroxylation of clay minerals and/or decomposition of organic matter present in these samples.

Table 3. Chemical composition of clays (in % by mass)

Samples	SiO_2	Al_2O_3	K_2O	CaO	Ti_2O	Fe_2O_3	SiO_2/Al_2O_3	PF
AG-Kor	49.47	19.72	0.42	-	0.95	8.90	2.51	20.54
AG-Ya	66.01	11.30	1.08	0.04	1.30	6.29	5.84	13.97

X-ray diffraction (XRD) analyses have identified the main crystalline phases. **Figure 2** shows the diffractograms of the AG-Kor and AG-Ya clays. A superposition of the peaks on the 2 diffractograms is observed, which highlights a similarity between these two clays. Indexing of the diffractograms reveals that AG-Kor and AG-Ya are composed of kaolinite ($Al_2Si_2O_5(OH)_4$) and illite ($KAl_2(Si_3Al)O_{10}(OH)_2$) as clay minerals, associated with quartz (SiO_2), iron compounds (goethite (α-FeOOH) and hematite (α-Fe_2O_3)) and rutile (TiO_2).

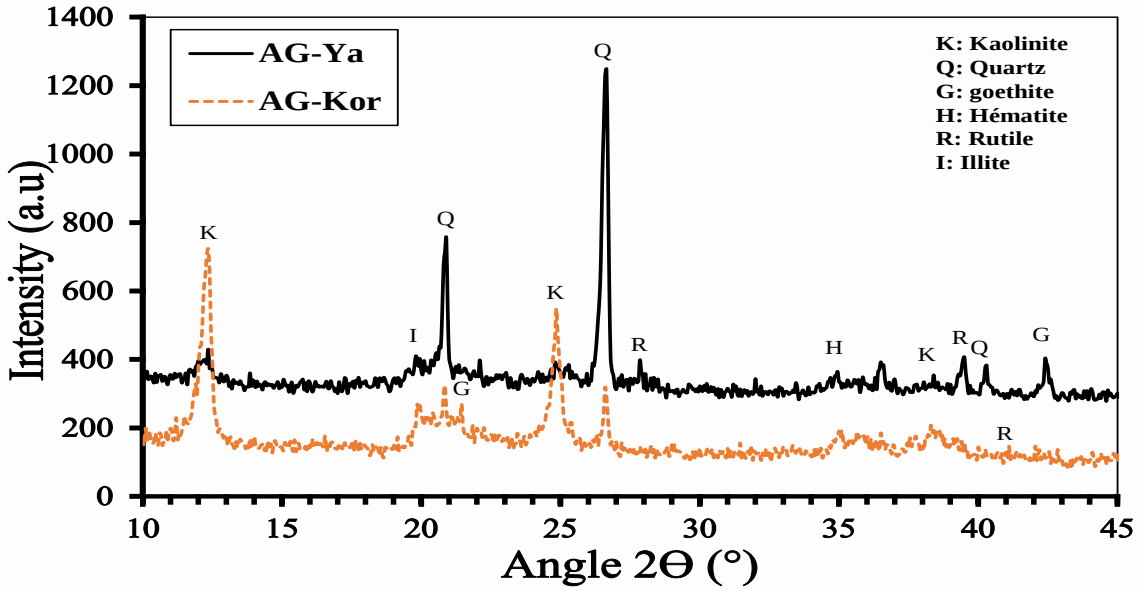

Figure 2. X-ray diffractograms of AG-Kor and AG-Ya

These results of ray diffraction and those of chemical composition, were used to estimate the semi-quantitative mineralogical composition presented in **Table 4.**

Table 4. Semi-quantitative mineralogical composition

Samples	Kaolinite	Illite	Quartz	Rutile	Hématite+ Goethite	Total
AG-Kor	47.15	4.57	25.07	0.95	8.9	86.64
AG-Ya	21.53	11.74	49.71	1.3	6.3	90.58

The results show the predominance of clay minerals (kaolinite and illite) with 51.72% for AG-Kor and 33.27% for AG-Ya, along with quartz, representing 25.07% and 49.71% in AG-Kor and AG-Ya, respectively. In addition, a moderate amount of iron compounds (hematite and goethite) is also present. The colour observed for each sample is related to the oxidation state of the iron it contains. The red and yellow colours observed in AG-Kor and AG-Ya, respectively, indicate the presence of oxidized iron (Fe III) (Coulibaly *et al*., 2014). The reddish color of the AG-Kor sample is due to its higher content of iron compounds compared to AG-Ya.

Differential Thermal and Thermogravimetric Analyses (DTA/TGA) of the samples were conducted to understand their thermal behavior and transformations over a temperature range from 30 to 900 °C. **Figure 3** shows the thermogram of the samples. On the different thermograms, 4 zones can be identified:

- Zone 1 (30-130 °C): both samples undergo hygroscopic water departure. This loss of water leads to a decrease in mass of about 1% for the AG-Kor sample and 1.50% for AG-Ya. This endothermic phenomenon does not cause any modification to the crystalline structure of the material (Sei *et al*., 2002).

- Zone 2 (130–330 °C) : The thermograms of AG-Kor and AG-Ya show an endothermic peak around 300 °C. This phenomenon is accompanied by a mass loss of 0.97% for AG-Kor and 1.40% for AG-Ya, and is generally attributed to the dehydroxylation of goethite into hematite, as described by **Equation 2** below (Farmer and Russell, 1964) :

$$2FeOOH \rightarrow Fe_2O_3 + H_2O \qquad \textbf{Eqn. 2}$$

- Zone 3 (330–630 °C): An endothermic peak is observed at 502 °C on the thermogram of AG-Kor, accompanied by a mass loss of 10.15%, while for AG-Ya the peak appears at 480 °C with a mass loss of 4.26%. This endothermic phenomenon can be primarily attributed to the dehydroxylation of kaolinite (Doubi, 2013)**.** Indeed, during this dehydroxylation reaction, the structural hydroxyls are removed from the kaolinite and leads to the formation of an amorphous phase called metakaolinite (Bellotto *et al.*, 1995; Chen *et al.*, 2000)**.** The decomposition temperature is related to the experimental conditions and the origin of the material (Gniewek, 1987). The overall dehydroxylation reaction is given by **Equation 3** (Gridi-Bennadji, 2007).

$$Al_2Si_2O_5(OH)_4 \rightarrow Al_2O_3, 2SiO_2 + 2H_2O \qquad \textbf{Eqn.3}$$

The significant difference observed between the values of mass losses would be due to the proportion of kaolinite as revealed by the XRD (21.53% for AG-Ya and 47.15% for AG-Kor). For the same sample mass, the proportion of kaolinite in AG-Kor is almost double that of AG-Ya.

- Zone 4 (above 630 °C): The mass of both samples remains almost unchanged, stabilizing at 86.88% for AG-Kor and 91.97% for AG-Ya. This indicates the mass stability of both samples in this temperature range.

The results of the complementary analysis by infrared spectroscopy are shown in **Figure 4**. The combined IR spectra of the two samples exhibit the same absorption bands, similar to those typically observed in clay raw materials. The infrared spectra show the presence of vibration bands at 3695 cm^{-1} and 3620 cm^{-1}, which can be attributed to hydroxyl (OH) groups of kaolinite (Seynou, 2009; Sorgho, 2013). The band at 3620 cm^{-1} is also characteristic of the OH^- group in illites (Kouamé *et al.*, 2021). The band observed at 3695 cm^{-1} is attributed to the vibrations of external hydroxyl groups of the kaolinite (Saikia and Parthasarathy, 2010). However, the one observed at 3620 cm^{-1} corresponds to the hydroxyl groups internal to the sheets (Sorgho, 2013).

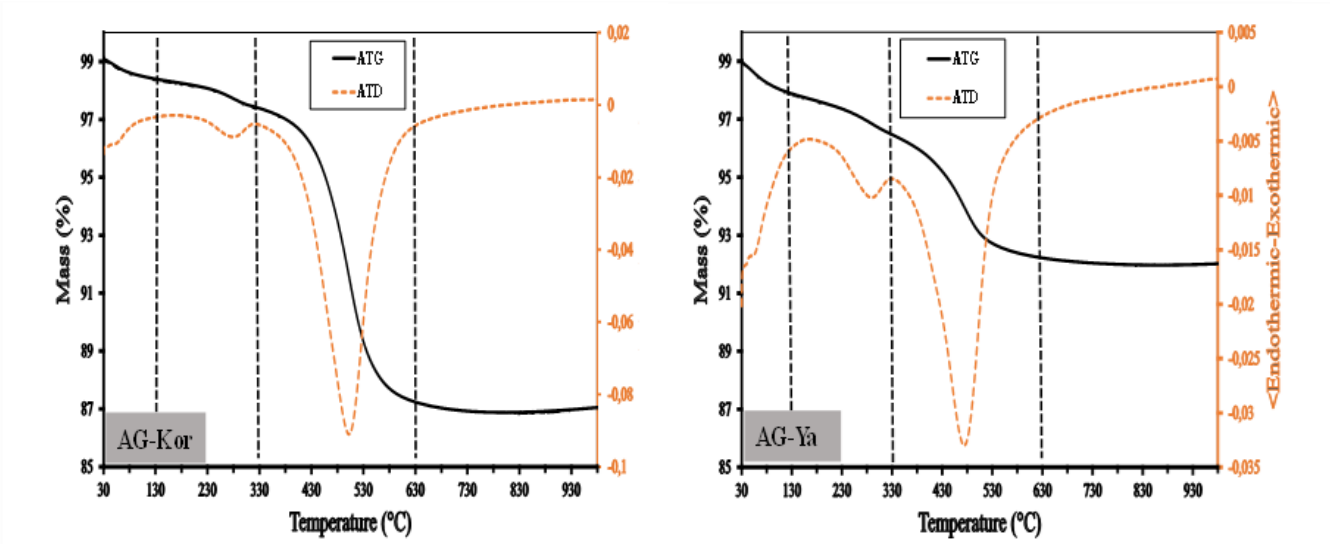

Figure 3. DTG/DTA thermograms of AG-Kor and AG-Ya

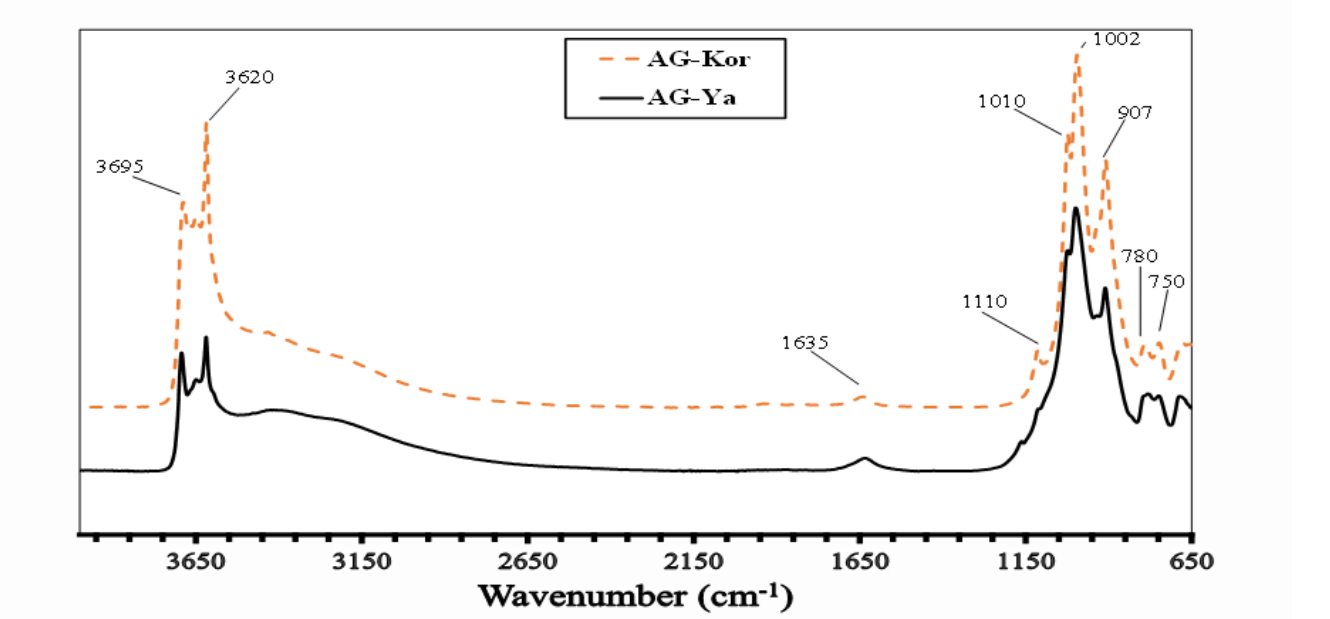

Figure 4. Infrared spectra of AG-Kor and AG-Ya

The band at 1635 cm^{-1} is attributed to the deformation vibrations of the water molecules adsorbed between the sheets (δH2O) (Abbès, 2017). Subsequently, the bands around 1110 and 1002 cm^{-1} are attributed to the stretching vibrations of the Si–O–Si bonds in kaolinite and illite, respectively, and to the Si–O bond vibrations in kaolinite (Saikia and Parthasarathy, 2010). As for the band at 907 cm^{-1}, it corresponds to the deformation vibrations of the Al-OH bonds in the kaolinite (Bich *et al.*, 2009).

Finally, the presence of quartz in both samples is evidenced by the band at 780 cm^{-1}. All the results are in agreement with those from X-ray diffraction, which showed that AG-Kor and AG-Ya are mainly composed of quartz and kaolinite. Scanning Electron Microscopy (SEM) was used to observe the morphology of the particles constituting the clay samples. The SEM images are shown in **Figure 5** below.

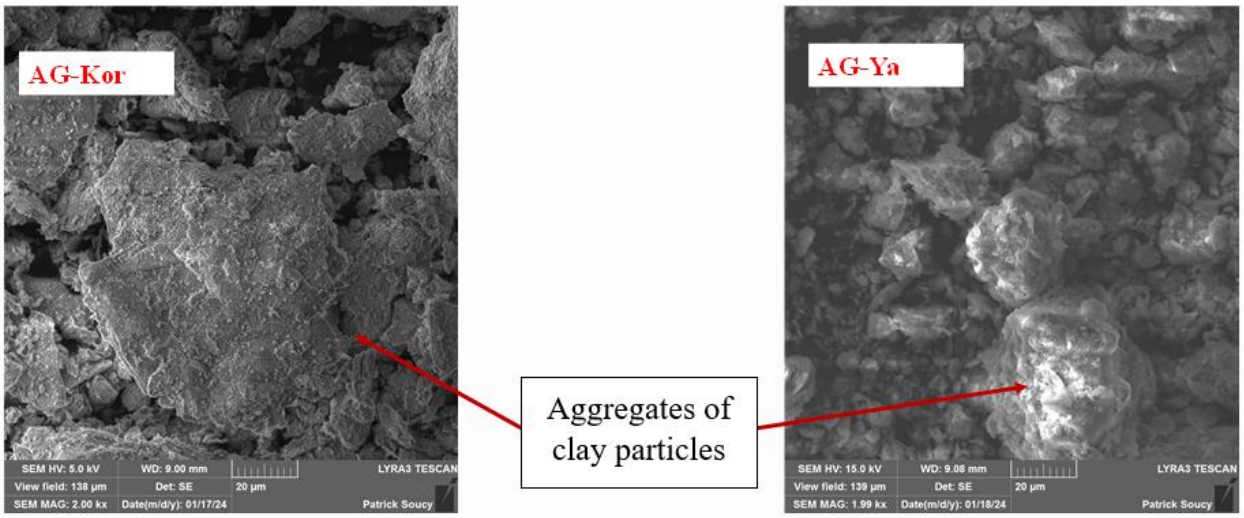

Figure 5. SEM images of AG-Kor and AG-Ya

These images were taken at different magnifications. These images show clearly visible aggregates of heterogeneous size mixed with small particles. The enlargement of these aggregates shows the presence of random stacks of sheets that could be kaolinite sheets.

The elemental chemical composition of the samples was determined using Energy Dispersive X-ray Spectroscopy (EDX). The EDX spectra of the AG-Kor and AG-Ya clays are shown in **Figure 6.** The EDX spectra of the AG-Kor and AG-Ya clays indicate that they are mainly composed of Fe, Ti, K, Si, Al, and O. This is agreement with the chemical composition determined by ICP, as well as with the composition of the various crystalline phases identified by XRD analysis. The most prominent peaks are attributed to Si, Al, and O.

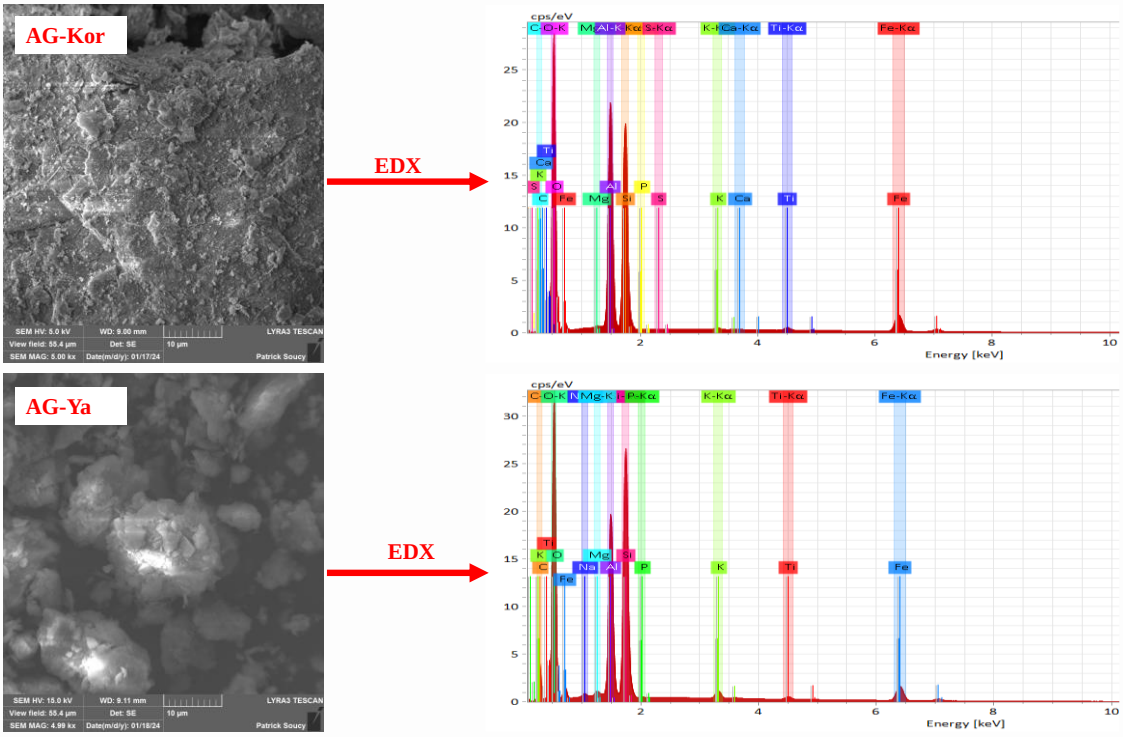

Figure 6. EDX spectra of AG-Kor and AG-Ya clays

Conclusion

The main objective of this study was to evaluate the physico-chemical and mineralogical properties of two local clays for their potential use in the treatment of wastewater from artisanal activities in the city of Korhogo, located in northern Côte d'Ivoire. The clays denoted AG-Kor and AG-Ya from Korhogo in the north and Yaou in the south of Côte d'Ivoire respectively were therefore characterized. Particle size analysis results showed that both samples are fine, with an average particle size of less than 1 µm. Specific surface areas of 42.04 and 33.68 m²/g were measured for AG-Kor and AG-Ya, respectively, along with a micropore percentage of around 72%. As for the physico-chemical and mineralogical characterization results, they showed that both clay samples are essentially composed of kaolinite (21.53% for AG-Ya and 47.15% for AG-Kor) and quartz (49.71% for AG-Ya and 25.07% for AG-Kor), along with associated iron compounds and rutile. Due to their composition and relatively high specific surface area, these two samples are chemically reactive and can therefore be used in adsorption processes for wastewater treatment.

References

Abbès B. (2017). *Absorption de composés organiques par la houille et la bentonite* [PhD Thesis]. Thèse de doctorat. 2017, 1-112, http://rdoc.univsba.dz/bitstream/123456789

Akartasse N., Azzaoui K., Mejdoubi E., Elansari L. L., Hammouti B., Siaj M., and Rhazi L. (2022). Chitosan-Hydroxyapatite Bio-Based Composite in Film Form: Synthesis and Application in Wastewater. *Polymers*, *14*, 4265. https://doi.org/10.3390/polym14204265

Ayari F., Srasra E., Trabelsi-Ayadi M. (2004). Application des modèles de Langmuir et Freundlich aux isothermes d'adsorption des métaux lourds par l'argile purifiée. In *Journal de Physique IV (Proceedings)* (Vol. 122, pp. 229-234). https://doi.org/10.1051/jp4:2004122035

Azzaoui K., Aaddouz M., Akartasse N., Mejdoubi E., Jodeh S., Hammouti B., and Algarra M. (2024). Synthesis of β-Tricalcium Phosphate/PEG 6000 Composite by Novel Dissolution/Precipitation Method: Optimization of the Adsorption Process Using a Factorial Design—DFT and Molecular Dynamic. *Arab J Sci Eng* 49, 711–732. https://doi.org/10.1007/s13369-023-08390-8

Balogoun, C. K., Bawa M. L., Osseni S., and Aina M. (2015). Préparation des charbons actifs par voie chimique à l'acide phosphorique à base de coque de noix de coco. *International Journal of Biological and Chemical Sciences*, *9*(1), 563-580. https://doi.org/10.4314/ijbcs.v9i1.48

Bellotto M., Gualtieri A., Artioli G., and Clark S. M. (1995). Kinetic study of the kaolinite-mullite reaction sequence. Part I : Kaolinite dehydroxylation. *Physics and Chemistry of Minerals*, *22*(4). https://doi.org/10.1007/BF00202253

Bensid N., Berredjem Y., Hattab Z., Djellabi R., Khiereddine O., Magri P., and Boulmokh A. (2016). Adsorption of benzoic and salicylic acids using sodium and intercalated bentonite in aqueous solution. *Sensor letters*, *14*(9), 872-882. https://doi.org/10.1166/sl.2016.3741

Bich C., Ambroise J., and Péra J. (2009). Influence of degree of dehydroxylation on the pozzolanic activity of metakaolin. *Applied Clay Science*, *44*(3-4), 194-200. https://doi.org/10.1016/j.clay.2009.01.014

Chen C.Y., Lan G.S., Tuan W.H. (2000). Microstructural evolution of mullite during the sintering of kaolin powder compacts. *Ceramics international*, *26*(7), 715-720. https://doi.org/10.1016/S0272-8842(00)00009-2

Coulibaly V., Sei J., Koffi L.K., Oyetola S., Jdid E.-A., and Thomas F. (2014). Mineralogical and chemical characteristics of clays consumed in the District of Abidjan (Côte D'Ivoire). *Materials Sciences and Applications*, *5*(14), 1048-1059. https://dx.doi.org/10.4236/msa.2014.514108

Deghles A., Hamed O., Azar M., Lail B. A., Azzaoui K., Obied A. A. and Jodeh S. (2019). Cellulose with Bidentate Chelating Functionality: An A Adsorbent for Metal Ions from Wastewater. *BioResources*. 14:3. http://dspace.pass.ps/handle/123456789/37

Farmer V. t, and Russell J. D. (1964). The infra-red spectra of layer silicates. *Spectrochimica acta*, *20*(7), 1149-1173. https://doi.org/10.1016/0371-1951(64)80165-X

Feller C., Schouller E., Thomas F., Rouiller J., and Herbillon A.J. (1992). N2-BET specific surface areas of some low activity clay soils and their relationships with secondary constituents and organic matter contents. *Soil Science*, *153*(4), 293-299. https://journals.lww.com/soilsci/toc/1992/04000

Gniewek J. (1987). Réactivité des montmorillonites calcinées : Utilisation dans le génie civil [PhD Thesis, ANRT]. https://pascal francis.inist.fr/vibad/index.php?action=get

Gridi-Bennadji F. (2007). Matériaux de mullite à microstructure organisée composés d'assemblage muscovite-kaolinite [PhD Thesis, Limoges]. https://theses.fr/2007LIMO4033

Hadjltaief H. B., Da Costa P., Beaunier P., Gálvez M. E., and Zina M. B. (2014). Fe-clay-plate as a heterogeneous catalyst in photo-Fenton oxidation of phenol as probe molecule for water treatment. *Applied Clay Science*, *91*, 46-54. https://doi.org/10.1016/j.clay.2014.01.020

Hamed O., Lail B. A., Deghles A., Qasem B., Azzaoui K., Obied A. A. and Jodeh S. (2019). Synthesis of a cross-linked cellulose-based amine polymer and its application in wastewater purification. *Environ Sci Pollut Res* 26, 28080–28091. https://doi.org/10.1007/s11356-019-06001-4

Jebahi S., Hidouri M., and Boughzala K. (2022). Kinetic and thermodynamic study of the retention of textile effluent by co-products from the phosphate industry. *RHAZES: Green and Applied Chemistry*, *14*, 76-94. https://doi.org/10.48419/IMIST.PRSM/rhazes-v14.31154

Jodeh S., Hamed O., Melhem A., Salghi R., Jodeh D., Azzaoui K., and Murtada K. (2018). Magnetic nanocellulose from olive industry solid waste for the effective removal of methylene blue from wastewater. *Environ Sci Pollut Res* 25, 22060–22074. https://doi.org/10.1007/s11356-018-2107-y

Kouadio L. M., Coulibaly Z., Kedi A. B. B., Coulibaly V., and Sei J. (2024). Capacity of two clays to clean up water from an illegal gold mining site. *European Journal of Applied Sciences*, *12*(3), 266-277. https://dx.doi.org/10.14738/aivp.123.16868

Kouamé A. N., Konan L. K., and Doubi B. I. H. G. (2021). Microstructure and mineralogy of compressed earth bricks incorporating shea butter wastes stabilized with cement. *Advances in Materials*, *10*, 67-74. https://doi.org/10.11648/j.am.20211004.13

Manouan W. M. R., Irié B., Kouakou P. M.-S., Kouamé A., Koffi, B., Kouamé A. N., and Méité N. (2024). Properties and Characterization of Two Clays Raw Material from Mountain District (West of Côte d'Ivoire) for Use in Low-Carbon Cements. *Advances in Materials Physics and Chemistry*, *14*(8), 137-145. https://doi.org/10.4236/ampc.2024.148011

Martinez A., Castro M., McCabe C. and Gil-Villegas A. (2007). Prédiction des isothermes d'adsorption à l'aide d'une théorie statistique bidimensionnelle des fluides associatifs. *Le Journal de physique chimique*, *126*(7). https://doi.org/10.1063/1.2483505

Méité N., Konan L.K., Tognonvi M.T., Doubi B.I.H.G., Gomina M., and Oyetola S. (2021). Properties of hydric and biodegradability of cassava starch-based bioplastics reinforced with thermally modified kaolin. *Carbohydrate Polymers, 254*, 117322. https://doi.org/10.1016/j.carbpol.2020.117322

Qlihaa A., Dhimni S., Melrhaka F., Hajjaji N., and Srhiri A. (2016). Caractérisation physico-chimique d'une argile Marocaine [Physico-chemical characterization of a morrocan clay]. *J. Mater. Environ. Sci*, *7*(5), 1741-1750.

Rache M. L., García A. R., Zea H. R., Silva A. M., Madeira L. M., and Ramírez J. H. (2014). Azo-dye orange II degradation by the heterogeneous Fenton-like process using a zeolite Y-Fe catalyst—kinetics with a model based on the Fermi's equation. *Applied Catalysis B: Environmental*, *146*, 192-200. https://doi.org/10.1016/j.apcatb.2013.04.028

Razzouki B., El Hajjaji S., Azzaoui K., Errich A., Lamhamdi A., Berrabah M., and Elansari L. L (2015). Physicochemical study of arsenic removal using iron hydroxide. *J. Mater. Environ. Sci.* 6 (5) (2015) 144-1450

Rodier J. (2005). L'analyse de l'eau naturelle, eaux résiduaires, eaux de mer. 8ème Edition DUNOD technique. *Paris.(P1008-1043)*.

Saikia B. J., and Parthasarathy G. (2010). Fourier transform infrared spectroscopic characterization of kaolinite from Assam and Meghalaya, Northeastern India. *J. Mod. Phys*, *1*(4), 206-210.

Sei J., Jumas J. C., Olivier-Fourcade J., Quiquampoix H., and Staunton S. (2002). Role of Iron Oxides in the Phosphate Adsorption Properties of Kaolinites From the Ivory Coast. *Clays and Clay Minerals*, *50*(2), 217-222. https://doi.org/10.1346/000986002760832810

Seynou M. (2009). Caractérisation de matières premières argileuses des sites de Loulouka et de Korona (Burkina Faso) : Valorisation dans la céramique du carreau [PhD Thesis]. Thèse de l'Université de Ouagadougou.

Sorgho B. (2013). Caractérisation et valorisation de quelques argiles du Burkina Faso : Application au traitement des eaux et aux géomatériaux de construction [PhD Thesis]. Thèse de Doctorat, Universite de Ouagadougou.

Soro N. S. (2003). Influence des ions fer sur les transformations thermiques de la kaolinite [PhD Thesis, Limoges]. https://theses.fr/2003LIMO0007

Ünnü B. A., Gündüz G., and Dükkancı M. (2016). Heterogeneous Fenton-like oxidation of crystal violet using an iron loaded ZSM-5 zeolite. *Desalination and Water Treatment*, *57*(25), 11835-11849.https://doi.org/10.1080/19443994.2015.1044915